for the more general case of mixtures of hard spheres.

[33]N. W. Ashcroft, Phys. Letters 23, 48 (1966).

[34]J. Hubbard, Proc. Roy. Soc. (London) A243, 336 (1957).

[35]G. A. Neece, F. J. Rogers, and W. G. Hoover (unpublished).

[36]H. D. Luedemann and G. C. Kennedy, J. Geophys. Res. 73, 2795 (1968).

[37]Handbook of Chemistry and Physics, 48th ed., edited by R. C. Weast (Chemical Rubber Co., Cleveland, Ohio, 1967).

[38]N. S. Gingrich and L. Heaton, J. Chem. Phys. 34, 873 (1961).

[39]V. V. Goldman, G. K. Horton, and M. L. Klein, Phys. Letters 28A, 341 (1968).

[40]E. G. Brovman, Yu. Kagan, and A. Kholas, Zh. Eksperim. i Teor. Fiz. 57, 1635 (1969) [Sov. Phys. JETP 30, 883 (1970)].

Pair Effects in Substitutional Alloys.
I. Systematic Analysis of the Coherent-Potential Approximation*

L. Schwartz

Division of Engineering and Applied Physics, Harvard University, Cambridge, Massachusetts 02138

and

E. Siggia†

Department of Physics, Harvard University, Cambridge, Massachusetts 02138

A single-band model is used to study the electronic structure of disordered binary alloys. Functional-derivative techniques are used to generate an expansion for the electron self-energy that is free of all "multiple-occupancy" corrections. This analysis reveals that the relevant small parameter for the coherent-potential approximation (CPA) is Z^{-1}, where Z is the number of nearest neighbors. In addition to being exact to first order in the concentration x and third order in the impurity potential δ, the CPA retains just those contributions of higher order in x and δ that are independent of Z^{-1}. Various methods have been suggested to calculate corrections to the CPA due to two-atom clusters. While all of these are exact to order x^2 and δ^5, we argue that a proper generalization of the CPA must also be correct to higher orders in Z^{-1}. The appropriate equations are derived and shown to imply the existence of satellite levels on either side of the impurity subband. A formalism is developed to examine the departure from the usual assumption of complete compositional disorder. To order x^2, the single-band Hamiltonian is found to imply the existence of short-range order in the alloy. The influence of this short-range order on the density of states is discussed and is shown to modify the clustering effects previously evaluated.

I. INTRODUCTION

This paper is concerned with the single-particle theory of the electronic structure of disordered binary alloys. The problem is most simply discussed in terms of a nearest-neighbor tight-binding-model Hamiltonian.[1,2] This model has the simplifying feature that the disordered potential is cell localized and may therefore be decomposed into a sum of contributions from each site. In a Wannier basis these contributions are simply the energy levels ϵ^A and ϵ^B of the two constituents. It is assumed that the distribution of these levels is completely random. A principal advantage of this model lies in the fact that there are available a number of exact results concerning the localization of the energy spectrum and the values of the leading moments of the density of states.[1] These exact results have been used to compare several common theories based on a "single-site" decoupling of the equations of motion. Following this course several authors[1-8] have concluded that the coherent-potential approximation (CPA) of Soven[3] and others provides the best possible single-site description of the alloy. Within the appropriate limits, the CPA exhibits dilute alloy, virtual crystal, and well-separated–impurity-band behavior.[1]

The coherent-potential (CP) concept has generally been developed within the framework of a multiple-scattering description of disordered systems.[1-3,8-12] In this approach the propagation of the electron is regarded as a succession of elementary atomic scatterings which are then averaged over all configurations of the alloy. The essential feature of the CPA is that the individual scatterers are viewed as being embedded in an effective medium whose choice is open and can be made self-consistently. This physical condition corresponding to this choice is simply that if the part of the medium belonging to a given site is removed and replaced by the true

atomic potential then on the average there should be no further scattering. The effective medium determined by this condition is equivalent to the electron self-energy in the CPA.

While the usual derivations[1-3] of the CPA are both physically appealing and mathematically concise, nevertheless several fairly obvious questions remain unanswered. In particular, what are the small parameters (of the theory) and in terms of these parameters, what are the leading corrections to the CPA? More specifically, is it possible to identify a parameter such that the CPA represents the first term in a systematic perturbation expansion based on this parameter?

In addition, one may question the assumed lack of short-range order in the alloy. If the model Hamiltonian is treated carefully, there will exist correlations in the positions of the atomic scatterers. Physically, this short-range order reflects an attempt of the ions to adopt a configuration of minimum free energy when the alloy is annealled in thermal equilibrium. At what level of approximation must these correlation effects be taken into account if we are to obtain a consistent description of the electronic structure of the alloy?

Within the context of the tight-binding model the entire behavior of the Hamiltonian is specified in terms of just two parameters, x and δ, respectively, characterizing the concentration of impurities and the strength of their potentials. Since the CPA has been shown to interpolate between the virtual-crystal and split-band limits, it is clearly not an approximation based on weak impurity scattering. Nor is the CPA simply a low-density approximation. For, while it is true that the CPA is exact to only first order in x, it nevertheless gives better results than several other methods that are also accurate to order x.

Statements about the expansion parameter of the theory may be made most precisely in terms of the moments of the electronic density of states. The essential point is that in addition to x and δ, the moments depend on the hidden geometrical parameter Z^{-1}, where Z is the number of nearest neighbors.[13] Z^{-1} governs the size of the corrections to the CPA moments and is, in fact, the relevant expansion parameter of the thoery. In addition to the terms of order x, the CPA includes all contributions of order x^2, x^3, ..., and higher power of δ that are independent of Z^{-1}. It is precisely these terms that allow the CPA to predict so many moments exactly. More important, the parameter Z^{-1} scales down the corrections to the CPA. Accordingly, the errors in the CPA moments are $O(x^2/Z^2)$ rather than simply $O(x^2)$.

To establish the connection between the CPA and the parameters x and Z^{-1}, procedures based on arbitrary decouplings of the equations of motion must be replaced by systematic perturbation theory. In Sec. II, the functional derivative techniques of Martin and Schwinger[14] are used to derive a compact diagrammatic representation for the electron self-energy V. The principal advantage of the functional derivative method lies in the fact that it automatically includes the "multiple-occupancy corrections" that complicated previous diagrammatic expansion.[5-7]

The perturbation series expresses the various contributions to the self-energy in terms of x, δ, and the Wannier matrix elements $G(n, n')$ of the self-consistently determined Green's function. The latter quantities introduce the explicit dependence of V upon the energy z. Indeed, examination of the asymptotic behavior (as $z \to \infty$) of $G(n, n')$ allows us to immediately classify each diagram according to which moments of the self-energy it will contribute. These considerations also lead to an appreciation of the importance of the parameter Z^{-1}. Different matrix elements of G are asymptotically related to different powers of z and Z^{-1}. For example, as $z \to \infty$ the diagonal matrix element $G(n, n) \to z^{-1}$. By contrast if n and n' are nearest neighbors, $G(n, n') \to Z^{-1} z^{-2}$. It is then shown that the CPA incorporates every diagram that involves only the diagonal part of G. These are the most significant contributions in the sense that they lead to exact agreement for the leading moments of V (i.e., they exhaust the lowest-order sum rules). In addition, the errors in the higher CPA moments are small and are, in fact, no greater than x^2/Z^2. To illustrate these formal considerations, we present numerical results based on three different low-density approximations. Of the three methods, only the CPA provides an adequate description of the electronic density of states over the entire range of impurity strengths.

It must be emphasized that Z^{-1} is a relevant small parameter only for the *moments* of the self-energy and density of states. In particular, this parameter does not allow us to make any specific statements about the validity of the CPA at a given energy within its allowed spectrum or at the band edges. Statements about moments provide *necessary* conditions for an approximation to be accurate but they are by no means *sufficient*.

Having established that the parameter Z^{-1} provides a criterion for distinguishing between different methods all of which are exact to the same order in x, the CPA may be extended (Sec. III) to higher orders in x and Z^{-1}. At the next level, these results provide the best possible treatment of two-atom clusters just as the CPA was the best treatment of one-atom (i.e., single-site) clusters. The most obvious consequence of these pair clusters is the appearance of satellite levels on either side of the impurity subband. These levels may be interpreted as the bonding and antibonding states of

a two-atom "molecule" imbedded in an effective medium. This point of view will be considered in more detail in the second paper of this series where equivalent results will be derived from multiple-scattering theory.

The questions involving short-range order are discussed briefly in Sec. IV. To be consistent in the treatment of pair effects, one must take account of the fact that to order x^2 there exist induced correlations in the positions of the atomic constituents. When the formalism is generalized to include atomic correlations, it is found that to $O(x^2)$ the short-range order introduces no new qualitative features but does lead to a modification of the size of the clustering effects calculated in Sec. III.

It should be emphasized that this discussion of short-range order is limited to the tight-binding localized perturbation model and is included only for the sake of completeness. All effects related to the self-consistent choice of potentials (for example, charge transfer and the deformation of the unit cell) have been neglected. These effects are expected to contribute to the atomic correlations in a more fundamental way than they do to the electronic structure.

II. PERTURBATION THEORY AND SINGLE-SITE APPROXIMATION

A. Formulation of Problem

Consider the alloy to be described in the tight-binding representation. A single orbital $|n\rangle$ is associated with each site n. In second-quantized form the one-electron Hamiltonian is

$$H = \sum_n \psi_n^* \epsilon_n \psi_n + \sum_{n \neq m} \psi_n^* h_{nm} \psi_m , \qquad (2.1)$$

$$H = D + W . \qquad (2.2)$$

The second line defines the separation of H into a diagonal part D and an off-diagonal part W. The diagonal elements ϵ_n may be regarded as random atomic levels which assume one of two possible values ϵ^A or ϵ^B depending on whether an atom of type A or B occupies the site n. The respective concentrations of A and B atoms are x and $y \equiv 1 - x$, both varying from 0 to 1. The hopping integrals h_{nm} are assumed to be independent of the alloy configuration. The operator W may therefore be interpreted as the Hamiltonian of the pure crystal for which $\epsilon^A = \epsilon^B = 0$.

If we assume that only hopping between nearest neighbors is important, the matrix elements of W in the Bloch representation are

$$\langle k | W | k' \rangle = \delta_{kk'} (Zh) s(k) , \qquad (2.3)$$

$$\langle k | W | k' \rangle = \delta_{kk'} w \, s(k) . \qquad (2.4)$$

$s(k)$ describes the k dependence of the band energy, Z is the number of nearest neighbors, and $w \equiv Zh$ is one-half the bandwidth. In a simple-cubic crystal with lattice constant a, $s(k)$ takes the form

$$s(k) = -\tfrac{1}{3} (\cos k_x a + \cos k_y a + \cos k_z a) \quad . \qquad (2.5)$$

It is convenient to redefine ϵ^A and ϵ^B in terms of w and to fix the zero of energy such that

$$\epsilon^B = 0, \quad \epsilon^A = \delta w . \qquad (2.6)$$

The second of these equations defines the dimensionless impurity strength δ. The energy w simply scales the entire Hamiltonian and will be set equal to unity. The model Hamiltonian is then completely specified by the three parameters x, δ, and $h = Z^{-1}$.

Assuming that the Hamiltonian (2.1) is valid at finite temperatures, the statistical properties of the alloy are described by the density matrix

$$\rho = e^{-\beta(H - \mu^A N^A - \mu^B N^B)} / \mathrm{Tr}[e^{-\beta(H - \mu^A N^A - \mu^B N^B)}]$$

$$= e^{-\beta[H - (\mu^A - \mu^B) \sum_n \epsilon_n / \delta - \mu^B N]} /$$

$$\mathrm{Tr}[e^{-\beta(H - (\mu^A - \mu^B) \sum_n \epsilon_n / \delta - \mu^B N)}] . \qquad (2.7)$$

Here μ^A and μ^B are the chemical potentials of the two types of atoms, $N = N^A + N^B$ is the total number of electrons, and the trace extends over both the electron and configurational variables. The ensemble average of any observable A, to be denoted by $\langle A \rangle$ is defined as

$$\langle A \rangle \equiv \mathrm{Tr}[\rho A] .$$

The density matrix (2.7) allows the A and B atoms to adjust their positions in order to minimize the total free energy of the alloy. Indeed, it will be seen in Sec. IV that Eqs. (2.1) and (2.7) imply the existence of short-range order in the arrangement of the atomic constituents. In this and Sec. III, the effects of short-range order will be neglected. This approximation is exact if the alloy is quenched after being annealed at infinite temperature. At zero temperature, the density matrix for the random alloy is given by the factorized form

$$\rho = |g\rangle \{ [\exp(u \sum_n \epsilon_n)] / \mathrm{Tr}[\exp(u \sum_n \epsilon_n)] \} \langle g| , \qquad (2.8)$$

where $u = -\beta(\mu^A - \mu^B)/2\delta$ and $|g\rangle$ is the unique ground state of the electron variables. The trace in (2.8) is over the possible values 0, δ, of ϵ_n, the configuration-independent characteristics of H having been incorporated into $|g\rangle$. The value u is fixed by the requirement

$$\langle \epsilon \rangle = \mathrm{Tr}[\rho \epsilon_n] = x\delta . \qquad (2.9)$$

There are several techniques in terms of which one may develop a perturbative expansion for the one-electron properties of the alloy. Adopting the

functional-derivative approach of Martin and Schwinger,[14] we allow the parameter u in (2.8) to vary from site to site

$$\rho = |g\rangle \{ [\exp(\textstyle\sum_n u_n \epsilon_n)] / \mathrm{Tr}\,[\exp(\textstyle\sum_n u_n \epsilon_n)] \} \langle g | \ .$$

(2.10)

The site dependence of u_n is simply a formal device, at the end of any calculation all the u_n will be set equal as in (2.8) and (2.9). Various quantities of interest may now be derived by differentiation with respect to u_n. For example, the connected correlation functions, describing fluctuations in the disordered potentials, are defined as

$$C(n_1, \ n_2, \cdots, n_l) = \frac{\delta^l}{\delta u_l \cdots \delta u_2} \langle \epsilon_{n_1} \rangle$$

$$= \frac{\delta^l}{\delta u_l \cdots \delta u_1} \ln \mathrm{Tr}[\exp(\textstyle\sum_n u_n \epsilon_n)] \ . \quad (2.11)$$

The first few of these functions are

$$C(n_1, \ n_2) = \langle \epsilon_1 \epsilon_2 \rangle - \langle \epsilon_1 \rangle \langle \epsilon_2 \rangle \ ,$$

$$C(n_1, \ n_2, \ n_3) = \langle \epsilon_1 \epsilon_2 \epsilon_3 \rangle - \langle \epsilon_1 \rangle \langle \epsilon_2 \epsilon_3 \rangle$$

$$- \langle \epsilon_2 \rangle \langle \epsilon_1 \epsilon_3 \rangle - \langle \epsilon_3 \rangle \langle \epsilon_1 \epsilon_2 \rangle + 2 \langle \epsilon_1 \rangle \langle \epsilon_2 \rangle \langle \epsilon_3 \rangle \ ,$$

etc. In the random alloy $C(n_1 \cdots n_l)$ is site diagonal and may be written as

$$C(n_1, \cdots, n_l) \to C^{(l)}_{n_1} = \delta_{n_1 n_2} \cdots \delta_{n_1 n_l} \, c^{(l)}(x) \delta^l , \quad (2.12)$$

where $c^{(l)}(x)$ is a polynomial in x of degree l, the first few of which are given in Table I. These polynomials are identical to the random-variable cumulants discussed by Leath,[15] Yonezawa,[5] and Kubo.[16] From Eqs. (2.11) and (2.12) it is not difficult to show that the cumulants may be derived from the generating relation

$$c^{(l)}(x) = \frac{d^l}{dt^l} \ln[xe^t + (1 - x)]\Big|_{t=0} \ .$$

Within the one-electron approximation, all the macroscopic properties of interest are determined from the Green's function

$$G(n, n') = i \langle T[\psi(n), \ \psi^\dagger(n')] \rangle$$

$$= i\eta(t - t') \langle \psi(n) \psi^\dagger(n') \rangle - i\eta(t' - t) \langle \psi^\dagger(n') \psi(n) \rangle ,$$

(2.13)

where

$$\eta(x) = \begin{cases} 0 , & x < 0 \\ 1 , & x > 0 \end{cases} .$$

In these equations n is a combined time-site index [i.e., $\psi(n') = \psi_{n'}(t')$] and T denotes the usual fermion time ordering. We conclude this subsection by observing that G satisfies the identity

$$i \langle \epsilon_n T[\psi(n), \ \psi^\dagger(n')] \rangle = \langle \epsilon_n \rangle \, G(n, n') + \frac{\delta G(n, n')}{\delta u_n} \ .$$

(2.14)

B. Perturbation Theory

To derive an equation of motion for $G(n, n')$ we combine (2.14) with the time derivative of (2.13):

$$-i\frac{dG}{dt}(n, n') = \delta(t - t')\,\delta_{nn'} + \eta(t - t')\left\langle \frac{d\psi(n)}{dt}\,\psi^\dagger(n) \right\rangle$$

$$- \eta(t' - t)\left\langle \psi^\dagger(n')\,\frac{d\psi(n)}{dt} \right\rangle$$

$$= \delta(n - n') - \sum_{m \neq n} h_{nm}\, G(m, n') - i\langle \epsilon_n T[\psi(n), \ \psi^\dagger(n')] \rangle$$

$$= \delta(n - n') - \sum_{m \neq n} h_{nm}\, G(m, n')$$

$$- \langle \epsilon_n \rangle G(n, n') - \frac{\delta G(n, n')}{\delta u_n} \ . \quad (2.15)$$

The second step follows from the Heisenberg equation

$$\frac{d\psi(n)}{dt} = i[H, \psi(n)] = -i\left(\epsilon_n \psi(n) + \sum_{m \neq n} h_{nm}\, \psi(m) \right) .$$

It terms of the Fourier transform

$$G(n, n'|z) = \int e^{-iz(t-t')}\, G(n, n')\, d(t - t') ,$$

(2.15) becomes

$$\delta_{nn'} = (z - \langle \epsilon_n \rangle) G(n, n'|z)$$

$$- \sum_{m \neq n} h_{nm}\, G(m, n'|z) - \frac{\delta G(n, n'|z)}{\delta u_n} \ . \quad (2.16)$$

Suppressing the explicit z dependence and adopting the convention of implied summation over all internal indices, Eq. (2.16) may be rewritten as

$$G^{-1}(n, n') = z\,\delta_{nn'} - h_{nn'} - V(n, n') , \quad (2.17)$$

where

$$V(n, n') \equiv \langle \epsilon_n \rangle \delta_{nn'} + \frac{\delta G(n, m)}{\delta u_n}\, G^{-1}(m, n'). \quad (2.18)$$

Rather than work directly with the propagator G it is more convenient to derive a perturbation series for the self-energy operator $V(n, n')$. Combining Eq. (2.18) with the identity

$$\frac{\delta G(n, m)}{\delta u_n}\, G^{-1}(m, n') = -G(n, m)\, \frac{\delta G^{-1}(m, n')}{\delta u_n}$$

$$= G(n, m)\, \frac{\delta V(m, n')}{\delta u_n} \ ,$$

TABLE I. Random variable cumulants.

$c^{(1)} = x$
$c^{(2)} = xy$
$c^{(3)} = xy(y - x)$
$c^{(4)} = xy(1 - 6xy)$
$c^{(5)} = xy(y - z)(1 - 12xy)$

FIG. 1. Diagrams representing the first four terms in Eq. (2.24).

we obtain the closed functional equation

$$V(n, n') = \langle \epsilon_n \rangle \, \delta_{nn'} + G(n, m) \, \frac{\delta V(m, n')}{\delta u_n} \quad . \quad (2.19)$$

Equation (2.19), the central result of this subsection, can be used to generate a systematic expansion for $V(n, n')$. To lowest order we have

$$V(n, n') = \langle \epsilon_n \rangle \, \delta_{nn'} \quad , \quad (2.20)$$

the usual "virtual-crystal" approximation. Subsequent terms in the perturbation series are derived by simple iteration of (2.19). For example, substitution of (2.20) into the second term on the right-hand side of (2.19) yields

$$V(n, n') = \langle \epsilon_n \rangle \, \delta_{nn'} + G(n, m) \, (\delta \langle \epsilon_m \rangle / \delta u_n) \, \delta_{mn'}$$

$$= \langle \epsilon_n \rangle \, \delta_{nn'} + G(n, n') \, C_n^{(2)} \delta_{nn'}$$

$$= [x\delta + xy \, \delta^2 \, G(n, n)] \, \delta_{nn'} \quad . \quad (2.21)$$

This result provides an adequate description of the electronic properties of the alloy in the weak-coupling limit $\delta \ll 1$, but is incapable of predicting the transition to a split-band regime as δ increases.

If δ may no longer be regarded as a small parameter then the interaction of (2.19) must be carried to completion. The parameters x and Z^{-1} can then be used to establish criteria for the selective summation of various terms to all orders in δ. The essential details are illustrated by the evaluation of the next contribution to $V(n, n')$. Substituting (2.21) into (2.19) we obtain

$$V(n, n') = \langle \epsilon_n \rangle \, \delta_{nn'} + G(n, m)(\delta / \delta u_n)$$

$$\times [\langle \epsilon_m \rangle + C_m^{(2)} \, G(m, m)] \, \delta_{mn'}$$

$$= \langle \epsilon_n \rangle \delta_{nn'} + G(n, m) [C_m^{(2)} \, \delta_{mn'} + C_m^{(3)} \, G(m, m) \, \delta_{mn}$$

$$+ C_m^{(2)}(\delta G(m, m) / \delta u_n)] \, \delta_{mn'} \quad . \quad (2.22)$$

To evaluate the last term in the square bracket of (2.22) we recall

$$\delta G(m, m) / \delta u_n = G(m, \overline{m}) \, (\delta V(\overline{m}, \overline{n}) / \delta u_n) \, G(\overline{n}, m)$$

$$\simeq G(m, n) \, C_n^{(2)} G(n, m) \quad . \quad (2.23)$$

Combining (2.23) and (2.22), we obtain the next approximation to the self-energy:

$$V(n, n') = [\langle \epsilon_n \rangle + C_n^{(2)} G(n, n) + G(n, n) \, C_n^{(3)} \, G(n, n)]\delta_{nn'}$$

$$+ G(n, n') \, C_{n'}^{(2)} G(n', n) \, C_n^{(2)} G(n, n') \quad . \quad (2.24)$$

The last term in this equation provides the leading contribution to the off-diagonal part of $V(n, n')$. Formally, these off-diagonal terms arise when $\delta / \delta u_n$ acts on matrix elements of G.

It is convenient to represent the various contributions to $V(n, n')$ diagramatically. To each factor $C_n^{(l)}$ we assign a cross with l dashed vertical lines emanating from it. The cross represents the cumulant $c^{(l)}(x)$ and the dashed lines are simply factors of δ. The matrix elements $G(n, n')$ will be depicted as solid horizontal lines, the ends of which are connected to potential (dashed) lines associated with $C_n^{(l)}$ and $C_{n'}^{(l')}$. The diagrams representing the four terms in (2.24) are shown in Fig. 1. It should be noted that the last term is at least $O(x^2)$ because it involves two factors of $c^{(2)}$. By contrast, the first three terms are all $O(x)$.

The remaining terms in the perturbation series are generated by further iteration of (2.19). Results up to sixth order in δ are summarized in Fig. 2. The three columns in this figure contain diagrams of order x, x^2, and x^3, respectively. Because each cross represents the cumulant $c^{(l)}(x)$ rather than simply a factor of x, our diagrams automatically include the "multiple-occupancy" corrections that enter other formulations of perturbation theory.[5-7] The connection between multiple occupancy and cumulants has been discussed by Yonezawa.[5] A principal advantage of the functional-derivative technique is that the cumulants emerge naturally, rather than via the complicated regrouping of terms discussed by Yonezawa.

In addition to the concentration x, the diagrams in Fig. 2 may be classified according to their dependence on the parameter Z^{-1}. This connection is made most directly in terms of the moments of $V(n, n')$:

$$\Lambda_{nn'}^{(p)} = \int_{-\infty}^{\infty} E^p \, \mathrm{Im} V(n, n') \, dE \quad . \quad (2.25)$$

For small p, $\Lambda_{nn'}^{(p)}$ may be evaluated exactly from the asymptotic expansion

$$V(n, n') = \langle \epsilon_n \rangle \, \delta_{nn'} + \sum_{p=0}^{\infty} \Lambda_{nn'}^{(p)} \, z^{-(p+1)} \quad . \quad (2.26)$$

Accordingly, the sequence of numbers $\Lambda_{nn'}^{(p)}$ furnish a criteria in terms of which we can distinguish between various approximate calculations of $V(n, n')$.

The z (and Z) dependence of $V(n, n')$ enters the perturbation theory through the factors of $G(n, n')$. The leading contributions as $z \to \infty$ are

$$G(n, n') = \langle n | \, (z - W - V)^{-1} \, | n' \rangle \quad , \quad (2.27a)$$

$$G(n, n') \sim z^{-1} \quad (n = n') \quad , \quad (2.27b)$$

$$G(n, n') \sim z^{-2} \, Z^{-1} \quad (n, n' \text{ nearest neighbors}) \quad . \quad (2.27c)$$

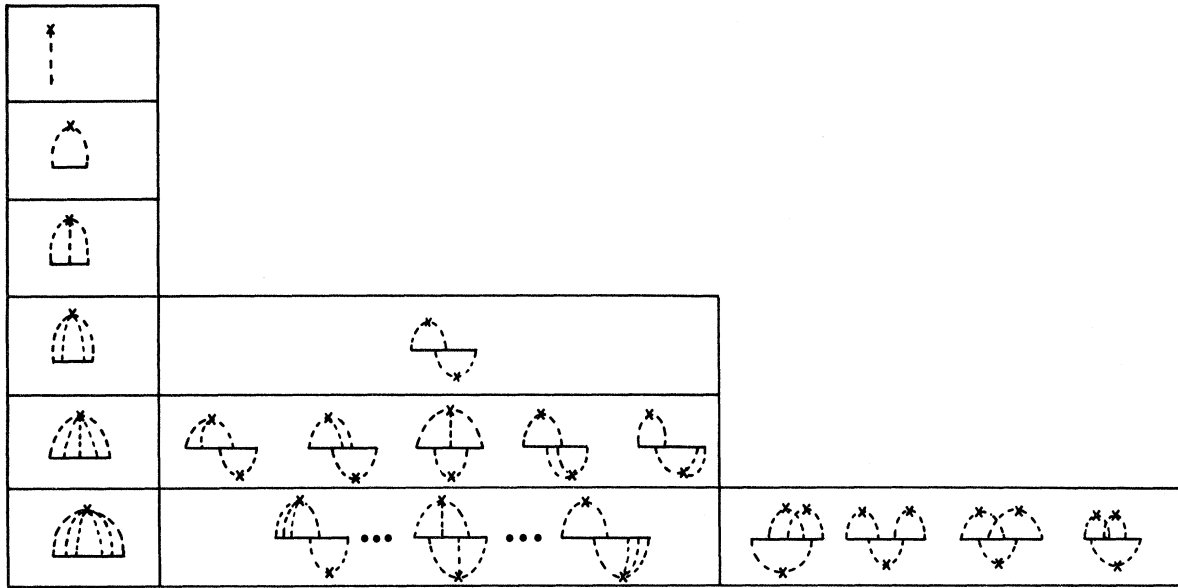In the last step we have used the fact that $\langle n | W | n' \rangle = h = Z^{-1}$.

FIG. 2. Self-energy diagrams through sixth order in δ.

If n and n' are separated by more than the nearest-neighbor distance, $G(n, n')$ is asymptotically higher order in z^{-1} and Z^{-1}. The exact coefficients depend on the specific type of crystal lattice.

Several conclusions follow immediately from Eqs. (2.27). First, in a given row of Fig. 2 the off-diagonal matrix elements of $V(n, n')$ are seen to affect only the higher moments of V, because they involve at least three powers of $G(n, n')$. In addition, because of the factors of Z^{-1} in (2.27c), their contribution is considerably smaller than that of the diagrams in the first column (all of which are independent of Z). Finally, we note that the diagrams in the nth ($n > 1$) column of Fig. 2 are all $O(x^n)$ but, in general, contain various powers of Z^{-1}. Consider, for example, the two diagrams shown in Fig. 3. If n and n' coincide, the first diagram involves only $G(n, n)$ and is independent of Z. If n' is one of the nearest neighbors of n, the net contribution from the Z diagrams of type (a) is $O(Z \cdot Z^{-3}) = O(Z^{-2})$. The second diagram in Fig. 3 requires an internal sum over m, and the contributions from different shells of neighbors are of varying orders in Z^{-1}. In both (a) and (b), the contributions of more distant neighbors are no greater than $O(Z^{-4})$, but the specific results depend on the type of lattice. These considerations illustrate that the dependence of a given diagram on Z^{-1} is a function of the number of distinct sites involved and of the distances between them.

Having classified the various contributions to $V(n, n')$ according to the parameters x, δ, and Z^{-1}, we can now consider different partial summations

of the perturbation series. The simplest of these is derived by approximating $c^{(1)}(x) \to x$ and summing the first column in Fig. 2. $V(n, n') \equiv V \, \delta_{nn'}$ is then given by

$$V = \frac{x\delta}{1 - \delta F} = xt ,$$　　　　　(2.28)

where

$$F \equiv G(n, n)$$　　　　　(2.29)

and t is the usual scattering operator for the potential δ. A somewhat better approximation is obtained by replacing $c^{(1)}(x)$ by $xy^{(1-1)}$:

$$V = \frac{x\delta}{1 - y\delta F} = \frac{xt}{1 + xtF} .$$　　　　　(2.30)

In both (2.28) and (2.30), $F(z)$ is related to the true propagator G and must therefore be calculated self-consistently in terms of V. In terms of the unperturbed propagator $G^{(0)} = (z - W)^{-1}$, the relation between $F(z)$ and V is simply

FIG. 3. Typical diagrams from the second column of Fig. 2. All such diagrams include contributions that are independent of Z^{-1}. This contribution arises when $n' = n$ in (a) and (b), respectively.
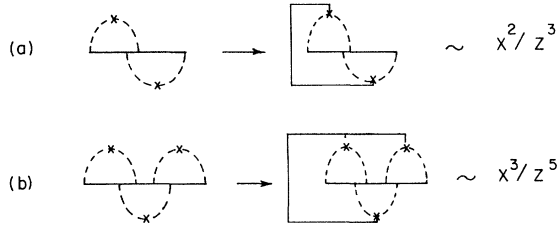
FIG. 4. Two contributions from the second and third columns of Fig. 2 that are retained by the CPA. When all sites are equal, the diagrams involve only $G(n, n)$. Accordingly, (a) and (b) contribute to the third and fifth moments of V, respectively.

$$F(z) = \langle n | [z - V - W]^{-1} | n \rangle = F^{(0)}(z - V). \qquad (2.31)$$

Equations (2.28) and (2.30) are appropriate for dilute alloys with moderate impurity strengths. If however δ is large enough to produce a separate impurity subband, these equations have important deficiencies. In particular, it will be seen that the shape of the minority subband is given incorrectly by these approximations.

Recently, several authors[1-5] have proposed a new method, the coherent-potential approximation (CPA), for the calculation of V. This approach leads to excellent agreement with exact results for the moments of the self-energy and electronic density of states. As in (2.28) and (2.30) the CP self-energy is site diagonal. The defining equation is

$$V = \frac{x\delta}{1 - (\delta - V)F} . \qquad (2.32)$$

In terms of the diagrams in Fig. 2, the CPA combines two principal contributions. First, all the diagrams in the first column are summed exactly (the cumulants are not approximated). Next, from the other columns we include the subset of crossed diagrams that have all their site indices equal. Two examples of this reduction are shown in Fig. 4. These two classes of diagrams comprise a complete solution of the alloy problem within the "single-site approximation," i.e., neglecting only contributions to V associated with off-diagonal matrix elements of $G(n, n')$. Perhaps the most elegant way to demonstrate that these diagrams are indeed equivalent to the CPA is to notice that iteration of the "single-site" version of (2.19)

$$V = \langle \epsilon \rangle + F \frac{dV}{du} , \qquad (2.33a)$$

together with the subsidiary condition

$$\frac{dF}{du} = F^2 \frac{dV}{du} , \qquad (2.33b)$$

generates precisely the diagrams we have just described. Equations (2.33) are a system of ordinary

differential equations whose solution is the CPA formula (2.32). The algebra required to verify this statement is presented in Appendix A.

The two classes of diagrams that enter the CPA can also be interpreted in terms of the "self-contained" cumulant formalism of Yonezawa.[5] Indeed, the self-contained cumulants $Q^{(l)}(x)$ are defined so that they already include the single-site contribution from the second, third, ... columns of Fig. 2. Accordingly in Ref. 5 the CPA is given directly as the sum of diagrams that are topologically identical to those in the first column but with $c^{(l)}(x)$ replaced by $Q^{(l)}(x)$:

$$V^{CPA} = \delta \sum_{l=1}^{\infty} Q^{(l)}(x) [\delta F(z)]^{l-1}.$$

Yonezawa's statement that in a proper single-site theory the bare cumulants $c^{(l)}(x)$ must be replaced by $Q^{(l)}(x)$ is then equivalent to our inclusion of selected contributions from the further columns of Fig. 2.

In view of this discussion it is clear why the CPA is the best of all "low-density" approximations. The CPA is exact to $O(x)$ [as are (2.28) and (2.30)] but in addition includes the most important contributions of order x^2, x^3,..., etc. The subset of diagrams retained from the further columns of Fig. 2 are precisely those that contribute to the leading moments of V. Note, for example, that the diagonal part of the first diagram in Fig. 4 is $O(x^2/z^3)$ while the Z off-diagonal parts are each $O(x^2/Z^3 z^6)$. The term included by the CPA contributes to the third moment of V while the neglected part influences only the sixth moment. In addition, because of the factors of Z, the errors in the higher moments are of order x^2/Z^2 rather than just x^2.

These considerations illustrate the importance of the parameter Z^{-1} in allowing us to distinguish between various approximations all of which are exact to the same order in x. While it is true that the CPA is a low-density (small-concentration) approximation, it is nevertheless a better approximation than (2.28) or (2.30) because it is also exact to $O(Z^{-1})$. To illustrate these conclusions we have performed numerical calculations based on three different low-density approximations. The three methods are the non-self consistent [i.e., $F(z) \rightarrow F^{(0)}(z)$] version of (2.30), a self-consistent treatment of (2.30), and the CPA [the differences between (2.30) and (2.28) are not great enough to warrant separate discussion of the latter equation]. In each case $F^{(0)}(z)$ was assumed to correspond to simple-cubic lattice with nearest-neighbor hopping. The relevant computational details have been discussed by Soven[2] and VKE[1] and need not be repeated here.

The results for the electronic density of states are shown in Fig. 5. Both the first approximation, usually referred to as the average-t-matrix approx-
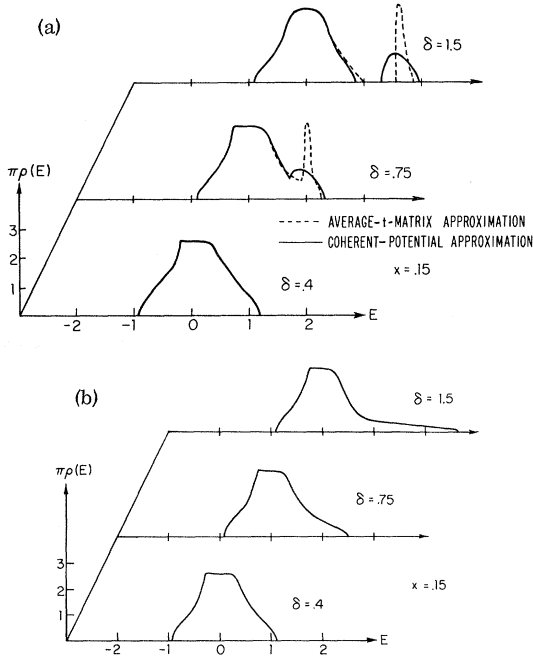
FIG. 5. (a) Comparison of density of states as calculated in the average t-matrix and coherent-potential approximations. (b) Density of states obtained by the self-consistent solution of (2.30).

imation[10,17-19] (ATA) and the CPA are seen to exhibit the development of increasing δ of the band shape from the virtual-crystal regime, through a stage in which the band is distorted at its upper edge, and finally to a stage in which it splits into independent subbands. By contrast, the self-consistent version of (2.30) is incapable of describing the transition to a split-band limit. The appearance of the true propagator $F(z)$ in (2.30) implies that all the internal propagation takes place in a medium that already has some impurity character. The interaction of the impurity potentials is therefore overestimated and the minority "subband" is too broad.

A more detailed study of Fig. 5(a) shows that while the locations and weights of the subbands are given correctly by both methods, the CPA describes their shape more correctly. In particular, the height and width of the CPA minority band both vary as $\sqrt{x}$ while in the ATA they vary as 1 and x, respectively. This difference is a reflection of the fact that four subband moments are given exactly by the CPA while only two are exact in the ATA.

To conclude, we emphasize that the main formal distinction between the three methods discussed above is their treatment of the parameter Z^{-1}. The ability of the CPA to describe the shape of the minority subband correctly is a direct consequence of the fact that it satisfies higher moments exactly. This is true because the CPA is the only approx-

imation that sums up all diagrams that refer to only a single site, i.e., all diagrams that are independent of Z^{-1}. It will be seen in Sec. III that these considerations are important in establishing the proper generalization of the CPA to higher orders in x and δ.

III. PAIR CORRECTIONS TO CPA

The techniques developed in Sec. II will now be used to examine the effects of two atom clusters. Various methods[6,8,20-22] have been proposed to deal with this problem. While all of these are exact to order x^2, they are not necessarily systematic in their treatment of the parameter Z^{-1}. The equations to be derived in this section are correct to second order in x and third order in Z^{-1}. These equations are then a proper generalization of the CPA in the sense that corrections to them are $Q(x^3/Z^4)$ rather than $O(x^3)$.

In Sec. II, the connection between the CPA and the diagrammatic expansion of the self-energy was ficilitated by the reduction of (2.19) to the single-site ordinary differential equation (2.33a). In the more general case no such formal device is available and we must return to the exact functional equation for $V(n, n')$. Equation (2.19) can be rearranged so that the CPA emerges as the lowest-order approximation rather than as a partial summation of the complete series. Once this is done, simple interation will generate the appropriate two-site equations.

To begin, we write (2.19) in the form

$$V(n, n') = \langle \epsilon_n \rangle \delta_{nn'} + G(n,\bar{n}) \frac{\delta}{\delta u_n} [V(\bar{n}, m) G(m, \bar{m})]$$

$$\times G^{-1}(\bar{m}, n') - G(n, \bar{n}) V(\bar{n}, m)$$

$$\times G(m, \bar{m}) \delta V(\bar{m}, n')/\delta u_n. \quad (3.1)$$

Equations (2.14) and (2.18) allow the second term on the right-hand side to be rewritten as

$$(\delta/\delta u_n)[V(\bar{n}, m) G(m, \bar{m})]$$

$$= i (\delta/\delta u_n) \langle \epsilon_{\bar{n}} \; T[\psi(\bar{n}), \psi^\dagger(\bar{m})] \rangle$$

$$= -\langle \epsilon_n \rangle V(\bar{n}, m) G(m, \bar{m}) + i \langle \epsilon_n \epsilon_{\bar{n}} \; T[\psi(\bar{n}), \psi^\dagger(\bar{m})] \rangle.$$
$$(3.2)$$

Now if n and $\bar{n}$ coincide, so that $\langle \epsilon_n \epsilon_{\bar{n}} \rangle \rightarrow \langle \epsilon_n^2 \rangle = \delta \langle \epsilon_n \rangle$, we have

$$i \langle \epsilon_n^2 \; T[\psi(n), \psi^\dagger(\bar{m})] \rangle = i \delta \langle \epsilon_n T[\psi(n), \psi^\dagger(\bar{m})] \rangle$$

$$= \delta V(n, m) G(m, \bar{m}), \quad (3.3)$$

while for $n \neq \bar{n}$ the generalization of (2.14) is

$$i \langle \epsilon_n \epsilon_{\bar{n}} \; T[\psi(\bar{n}), \psi^\dagger(\bar{m})] \rangle = \langle \epsilon_{\bar{n}} \rangle \delta G(\bar{n}, \bar{m})/\delta u_n$$

$$+ \langle \epsilon_n \rangle \ V(\bar{n}, m) \ G(m, \bar{m}) + \delta^2 G(\bar{n}, \bar{m})/\delta u_n \delta u_{\bar{n}} \ .$$
$$(3.4)$$

Combining these equations we obtain the useful identity

$$i \langle \epsilon_n \epsilon_{\bar{n}} \ T[\psi(\bar{n}), \psi^\dagger(\bar{m})] \rangle = [\delta V(n, m) \ G(m, \bar{m})] \ \delta_{n\bar{n}}$$

$$+ [\langle \epsilon_{\bar{n}} \rangle \ \delta G(\bar{n}, \bar{m})/\delta u_n + \langle \epsilon_n \rangle \ V(\bar{n}, m) \ G(m, \bar{m})$$

$$+ \delta^2 G(\bar{n}, \bar{m})/\delta u_n \delta u_{\bar{n}}] (1 - \delta_{n\bar{n}}). \quad (3.5)$$

Substitution of (3.5) into (3.2) and then into (3.1) leads to an alternate version of the exact-functional equation for $V(n, n')$. After some straightforward but rather tedious algebra, this equation may be put in the form

$$V(n, n') = V_n^{(0)} \delta_{nn'} + \varphi_n^{-1} \sum_{\bar{n} \neq n} [G(n, \bar{n}) \ \delta V(\bar{n}, n')/\delta u_n$$

$$- G(n, n) \ V(n, \bar{n}) \ G(\bar{n}, m) \ \delta V(m, n')/\delta u_n], \quad (3.6)$$

where

$$V_n^{(0)} = \langle \epsilon_n \rangle [1 + V(n, n) \ G(n, n)] \ \varphi_n^{-1} \quad (3.7a)$$

and

$$\varphi_n = 1 - (\delta - \langle \epsilon_n \rangle - V(n, n)) \ G(n, n) \ . \quad (3.7b)$$

It should be noted that the lowest approximation to (3.6) namely $V(n, n') \rightarrow V_n^{(0)} \delta_{nn'}$ is equivalent to the CP equation (2.32). Because of the exclusions in the summation, the last term in (3.6) generates the corrections to the CPA that depend on the off-diagonal matrix elements of G. The simplest of these corrections, those associated with two atom clusters are of order x^2/Z^2 and x^2/Z^3. Equation (3.6) allows us to treat these pair effects exactly.

To begin, we note that the last term in (3.6) involves two powers of V and is at least of order x^3. This term need be retained only when $n' = m = n$ and its contribution is $O(x^3/Z^3)$. Equation (3.6) may then be replaced by

$$V(n, n') = V_n^{(0)} \delta_{nn'} + \varphi_n^{-1} \sum_{\bar{n} \neq n} [G(n, \bar{n}) \ \delta V(\bar{n}, n')/\delta u_n$$

$$- G(n, n) \ V(n, \bar{n}) \ G(\bar{n}, n) \ (\delta V(n, n)/\delta u_n) \ \delta_{nn'}]. \quad (3.8)$$

Approximating $V(n, n') \rightarrow V_n^{(0)} \delta_{nn'}$ on the right-hand side of this equation, the leading contribution to the off-diagonal part of the self energy is simply

$$V^{(1)}(n, n') = \varphi_n^{-1} \ G(n, n') \ \delta V_{n'}^{(0)}/\delta u_n \ .$$

The derivative of $V_n^{(0)}$ with respect to u_n is evaluated in Appendix B. The resulting expression for $V^{(1)}(n, n')$ is

$$V^{(1)}(n, n') = G(n, n') \ \Gamma_{nn'} C_n^{(2)} C_{n'}^{(2)} \ (\varphi_n \varphi_{n'})^{-2} \ , \quad (3.9)$$

where

$$\Gamma_{nn'} = G(n, n') \ G(n', n) \ (1 - \delta_{nn'}). \quad (3.10)$$

Similarly, the first correction to the diagonal

part of $V(n, n')$ is given by

$$V^{(1)}(n, n) = \varphi_n^{-1} \sum_{\bar{n} \neq n} [G(n, \bar{n}) \ \delta V^{(1)}(\bar{n}, n)/\delta u_n$$

$$- G(n, n) \ V^{(1)}(n, \bar{n}) \ G(\bar{n}, n) \delta V_n^{(0)}/\delta u_n]$$

$$\simeq \sum_{\bar{n} \neq n} (\varphi_n \varphi_{\bar{n}})^{-1} \ \Gamma_{n\bar{n}} \ \delta^2 V_n^{(0)}/\delta u_n \delta u_{\bar{n}}$$

$$\simeq \sum_{\bar{n} \neq n} \varphi_n^{-1} C_n^{(3)} \ C_{\bar{n}}^{(2)} \ \Gamma_{n\bar{n}}^2 (\varphi_n \varphi_{\bar{n}})^{-2} \ , \quad (3.11)$$

where terms of order x^3/Z^4 have been neglected. Equations (3.9) and (3.11) provide corrections to the CPA that are of order x^2/Z^2 and x^2/Z^3, respectively. These are in fact the only contributions to $V(n, n')$ through third order in Z^{-1}. There are however further terms of second order in x which must be taken into account in a complete two-site theory. The remaining x^2 terms are obtained by successive iteration of Eq. (3.8). For example, the next contribution to $V(n, n')$ is

$$V^{(2)}(n, n') = [\varphi_n^{-1} \ G(n, n') \ \delta V^{(1)}(n', n')/\delta u_n] (1 - \delta_{nn'})$$

$$+ \left(\sum_{\bar{n} \neq n} (\varphi_n \varphi_{\bar{n}})^{-1} \ \Gamma_{n\bar{n}} \ \delta^2 V^{(1)}(n, n)/\delta u_n \delta u_{\bar{n}} \right) \delta_{nn'}$$

$$= [G(n, n') \ \Gamma_{nn'}^2 \ C_n^{(3)} C_{n'}^{(3)} \ (\varphi_n \varphi_{n'})^{-3}] (1 - \delta_{nn'})$$

$$+ \left(\sum_{\bar{n} \neq n} \varphi_n^{-1} \ C_n^{(4)} \ C_{\bar{n}}^{(3)} \Gamma_{n\bar{n}}^3 \ (\varphi_n \varphi_{\bar{n}})^{-3} \right) \delta_{nn'} \ .$$

As these terms are of higher order in Z^{-1}, the correlation functions need only be treated exactly to order x^2. Approximating the cumulents $c^{(l)}(x)$ for $l \geq 4$ by

$$c^{(l)}(x) \rightarrow xy \ (y - x)^{(l-2)} \ , \quad (3.12)$$

the final expression for the two-site self-energy may be written as

$$V(n, n') = V_n^{(0)} \ \delta_{nn'} + V^{(1)}(n, n') + V^{(2)}(n, n') + \cdots$$

$$= V_n^{(0)} \delta_{nn'} + \left(\frac{x^2 y^2 \Delta^4 G(n, n') \Gamma_{nn'}}{1 - (y - x)^2 \Delta^2 \Gamma_{nn'}} \right) \ (1 - \delta_{nn'})$$

$$+ \left(\sum_{\bar{n} \neq n} \frac{x^2 y^2 (y - x) \Delta^5 \Gamma_{n\bar{n}}^2}{1 - (y - x)^2 \Delta^2 \Gamma_{n\bar{n}}} \right) \ \delta_{nn'} \ , \quad (3.13)$$

where we define

$$\Delta = \delta \varphi^{-1} = \delta [1 - (y\delta - V(n, n)) \ G(n, n)]^{-1}. \quad (3.14)$$

Equations (3.13) and (3.14) are the principal formal results of this subsection. In addition to the diagrams of the second column in Fig. 2 (which are included to orders x^2 and Z^{-3}), these equations also retain contributions of order x^n/Z^2 and x^n/Z^3 ($n = 3, 4, \cdots$) associated with diagrams in the further columns that involve only two independent sites. For example, if the first and second sites coincide, then the contribution from the third-order diagram in Fig. 6 is included in Eq. (3.13). As indicated in
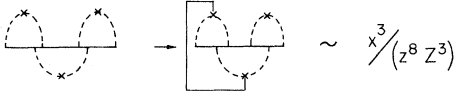
FIG. 6. A reduced third-order diagram whose contribution is retained by the two-site equations (3.13).

the figure, this type of restricted diagram influences the eighth moment of $V(n, n')$ and their net contribution (the second site may be any one of the Z neighbors of the first site) is $O(Zx^3/Z^3)$ $= O(x^3/Z^2)$. By contrast, when all three sites are distinct this diagram contributes to the tenth moment and is $O(x^3/Z^4)$. The present situation is then completely analogous to that encountered in Sec. II in connection with Fig. 4.

The derivation of the pair equations (3.13) requires the approximation (3.12). The behavior of the bare cumulants $c^{(l)}(x)$ for large l, as described by Yonezawa,[5] would seem to indicate that (3.12) is actually a rather poor approximation. However, in analogy with the single-site theory, the fact that Eqs. (3.13) retain all two-site contributions from the third, fourth, ... columns of Fig. 2 implies that the relevant quantities are the self-contained cumulants $Q^{(l)}(x)$ rather than the $c^{(l)}(x)$. Comparison of Figs. 6 and 10 of Ref. 5 reveals that $xy(y - x)^{(l-2)}$ is likely to be much better approximation to $Q^{(l)}(x)$ than it is to $c^{(l)}(x)$. Equations (3.12) then, when viewed as an approximation $Q^{(l)}(x)$, are quite reasonable.

In order to implement Eqs. (3.13) we must be able to calculate the matrix elements $G(n, n')$. These quantities are readily available if the self-energy is site diagonal and the operator W corresponds to the simple-cubic cosine-band model of Wolfram and Callaway.[23] Unfortunately, it is not possible to extend that procedure to the more general self-energy in (3.13) unless the off-diagonal elements are restricted to nearest neighbors. Within this approximation, the Bloch representation of the self-energy is simply

$$V(k) = v(z) + v_1(z)_s(k),   (3.15)$$

where $v(z) = V(n, n)$ and $v_1(z) = ZV(n, n')$ $(n, n'$ nearest neighbors. The matrix elements $G(n, n')$ are then given by

$$G(n, n') \equiv \int_{B.Z.} \frac{e^{k \cdot (R_n - R_{n'})}}{z - v - (1 - v_1)s(k)} \, d^3k$$

$$= \frac{i}{(1 - v_1)} G^{(0)} \left(\frac{(z - v)}{(1 - v_1)} \right) .   (3.16)$$

Equation (3.16) replaces the single-site result $G(n, n') = \langle n | G^{(0)}(z - v) | n' \rangle$. Combining Eq. (3.16) and (3.13) we obtain a system of two coupled equations to be solved self-consistently for V and G.

To illustrate the effects of nearest-neighbor impurity pairs the formalism of this section has been used to calculate corrections to the CP density of states. The new qualitative feature associated with the pair clusters is the appearance of satellite levels on either side of the minority band in the dilute split-band limit (i.e., $x \lesssim 0.10$ and $\delta \gtrsim 1.0$). Physically, these levels are associated with the bonding and antibonding states of a two-atom molecule embedded in the effective medium. This point of view will be discussed in more detail in the second paper of this series. It will be shown there that Eqs. (3.13) are, in fact, equivalent to the requirement[24]

$$0 = \sum_{n \neq m} \langle t^{(2)}(n, m) \rangle ,   (3.17)$$

where

$$t^{(2)}(n, m) = (v_n + v_m)[1 - G(v_n + v_m)]^{-1}$$

and

$$\langle n | v_n | n' \rangle \equiv \epsilon_n \delta_{nn'} - V(n, n') .$$

$t^{(2)}(n, m)$ is the scattering operator for a pair of atoms located at the sites n and m. Equation (3.17) is the obvious generalization of the CP equation $\langle t_n \rangle = 0$.

The minority subband density of states obtained from the pair (CP-2) Eqs. (3.13) and the single-site (CP-1) coherent potential Eq. (2.32) are compared in Fig. 7. This figure illustrates the behavior of the satellite levels as a function of increasing concentration at a fixed value of δ. In the dilute limit the satellite levels are split off from the central part of the impurity band. In addition, the pair theory predicts that the central portion is somewhat higher and narrower than the original CPA result. This modification is necessary as both theories are expected to give the same value for the third moment (i.e., moment of inertia)
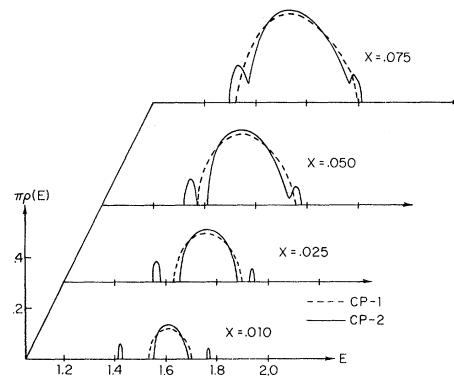

FIG. 7. Minority-band density of states as calculated from the single site (dash line) and pair (solid line) coherent-potential theories. The value of δ is 1.5.
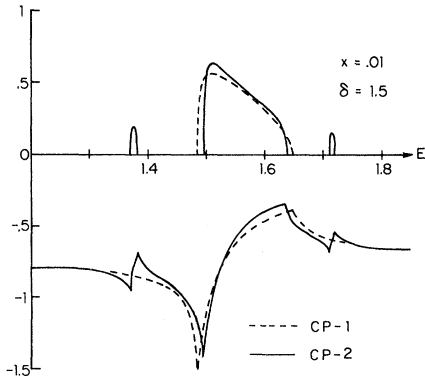
FIG. 8. Comparison of self-energy $V(n, n)$ in the minority band energy range.

of the subband density of states. Similar behavior is exhibited by the diagonal part of the self-energy. Figure 8 compares the CP-1 and CP-2 results for $V(n, n)$ in the energy range of the minority band. As the concentration of impurities is raised and the likelihood of hopping between them increased, the central part of the subband broadens and eventually merges with the satellite levels. The height and width of the satellite levels are seen to increase with concentration while their location is relatively unaffected.

Aside from these details of fine structure, the CP-2 equations lead to improved agreement with the exact moments of the density of states. The CP-1 gives the first eight moments of $\rho(E)$ exactly with corrections to the higher moments of order Z^{-2}, while the CP-2 gives at least twelve moments exactly with corrections that are $O(Z^{-4})$. Alternatively, it may be said that the CP-1 moments are exact to order x and retain all contributions of higher order in x and δ that are independent of Z^{-1}. Similarly the CP-2 moments are exact to order x^2 and include all higher contributions through third order in Z^{-1}. Formally these important contributions of higher order in x and δ enter the CP-2 equations via the factors of Δ in (3.13). Previous discussions of pair clustering have usually been based on a partial summation of the terms in the first two columns of Fig. 2. Approximating $c^{(1)}(x) \to x$ and summing this subclass of diagrams we obtain the result of Yonezawa and Matsubara[20] [their Eq. (3.15)]

$$V^{(2)}_{(n,n')} = xt + \left(\frac{x^2 t^4 G(n, n') \Gamma_{nn'}}{1 - t^2 \Gamma_{nn'}} \right) (1 - \delta_{nn'})$$

$$+ \left(\sum_{\bar{n} \neq n} \frac{x^2 t^5 \Gamma_{n\bar{n}}^2}{1 - t^2 \Gamma_{n\bar{n}}} \right) \delta_{nn'} , \qquad (3.18)$$

where $t \equiv \delta(1 - \delta G(n, n))^{-1}$ as in (2.28). In the dilute limit $(x \ll 1, y \to 1)$, Eqs. (3.13) and (3.18) are structurally identical except for the higher powers

of x and δ introduced by the replacement $t \to \Delta$. It is precisely these added contributions that allow the CP-2 to provide an improved treatment of the higher moments.

IV. SHORT-RANGE-ORDER EFFECTS

In this section we outline a procedure for calculating the correlations in the positions of the constituent atoms and for estimating their influence on the electron self-energy. It must be emphasized that these short-range-order effects are due entirely to the coupling of the ions implied by the Hamiltonian (2.1) and the density matrix (2.7).

We assume that the alloy has been annealed in thermal equilibrium at some elevated temperature T_a, not greater than the melting temperature. Adopting an imaginary time formalism, the electron field $\psi_n(\tau)$ is taken to depend on the real parameter τ in the interval $0 \leqslant \tau \leqslant \beta_a = (kT_a)^{-1}$. In an interaction representation the evolution in τ of $\psi_n(\tau)$ is governed by the equation

$$\frac{d\psi_n(\tau)}{d\tau} = [W, \psi_n(\tau)] = - \sum_{m \neq n} h_{nm} \psi_m(\tau) . \qquad (4.1)$$

Introducing the computational variables v_n, all of which will be set equal to δ at the end of the calculation, we rewrite the definition (2.2) as

$$D(\tau) = \sum_n \psi_n^\dagger(\tau) v_n \sigma_n \psi_n(\tau) , \qquad (4.2)$$

where $\sigma_n \equiv \epsilon_n / \delta$. The appropriate generalizations of (2.7), (2.13), and (2.19) are

$$\rho = \exp(-\beta_a W + \sum_n u_n \sigma_n) T[\exp(-\int_0^{\beta_a} D(\tau) d\tau)]/$$

$$Tr\{\exp(-\beta_a W + \sum_n u_n \sigma_n) T[\exp(-\int_0^{\beta_a} D(\tau) d\tau)]\} , \qquad (4.3)$$

$$G(n, n') = - Tr[\rho \psi_n(\tau) \psi_{n'}^\dagger(\tau')]$$

$$\equiv \beta_a^{-1} \sum_{p=-\infty}^{\infty} G(n, n' \mid \omega_p) e^{-\omega_p(\tau - \tau')} , \qquad (4.4)$$

and

$$V(n, n' \mid \omega_p) = v_n \langle \sigma_n \rangle \delta_{nn'} + v_n G(n, m \mid \omega_p)$$

$$\times \delta V(m, n' \mid \omega_p)/\delta u_n . \qquad (4.5)$$

The complex frequencies ω_p in the last part of (4.4) are defined as $\omega_p = \beta_a^{-1}(2p + 1)i$. As before, the final value of the parameters u_n is chosen so that

$$\langle \sigma_n \rangle_{\substack{v_n = \delta \\ u_n = u}} = x . \qquad (4.6)$$

In addition to the quantities described by Eqs. (4.3) to (4.5), it is convenient to introduce the auxiliary function

$$S(u, \delta) = Tr[\exp(-\beta_a W + \sum_n u_n \sigma_n) T$$

$$\times\{\exp[-\int_0^{\beta a} D(\tau)\,d\tau]\}]. \quad (4.7)$$

Iteration of Eq. (4.5) yields a system of diagrams that are formally identical to those in Fig. 2. The new feature of the present calculation is the fact that the correlation functions

$$C(n_1,\ldots,n_l)\equiv[\delta^l\ln S(u,\delta)/\delta u_1,\ldots,\delta u_l]\,\delta^l \quad (4.8)$$

are no longer diagonal. In particular, the leading effects of short-range order are contained in the off-diagonal part of $C(n,n')$. A perturbative calculation of $C(n,n')$ is carried our most easily in terms of the inverse matrix $\phi(n,n')$:

$$[C(n,n')]^{-1}\equiv(\langle\sigma_n\rangle-\langle\sigma_n\rangle^2)^{-1}\,\delta_{nn'}-\phi(n,n')$$
$$=(\delta\langle\sigma_{n'}\rangle/\delta u_n)^{-1}. \quad (4.9)$$

If $\phi(n,n')$ is small, the correlation between the sites n and n' is given by

$$C(n,n')=\langle\sigma_n\sigma_{n'}\rangle-\langle\sigma_n\rangle\langle\sigma_{n'}\rangle$$
$$=(\langle\sigma_n\rangle-\langle\sigma_n\rangle^2)\,\delta_{nn'}$$
$$+(\langle\sigma_n\rangle-\langle\sigma_n\rangle^2)\phi(n,n')(\langle\sigma_{n'}\rangle-\langle\sigma_{n'}\rangle^2), \quad (4.10)$$

and the enhanced probability that n' is occupied by an atom of type A given that n is so occupied is simply $xy^2\phi(n,n')$.

To derive a functional equation for $\phi(n,n')$ we begin with the differential form of (4.7)

$$\delta\ln S(u,\delta)=\langle\sigma_n\rangle\delta u_n-\beta_a\langle\psi^\dagger(n)\psi(n)\rangle\delta v_n. \quad (4.11)$$

Since $\langle\sigma_n\rangle=\delta\ln S/\delta u_n$, both S and ϕ may be viewed as functionals of $\langle\sigma_n\rangle$ and v_n. Accordingly, the Legendre transform of (4.11) is

$$\delta(\ln S(\langle\sigma\rangle,\delta)-\sum_n u_n\langle\sigma_n\rangle)$$
$$=-\sum_n(u_n\delta\langle\sigma_n\rangle+\beta_a\langle\psi^\dagger(n)\psi(n)\rangle\delta v_n).$$

Because this relation is exact, the cross derivatives of the coefficients on the right-hand side are equal. Differentiating the implied equation with respect to $\langle\sigma_{n'}\rangle$, we obtain

$$\frac{\delta\phi(n,n')}{\delta v_m}=-\sum_{\omega_p}e^{\omega_p 0^+}\frac{\delta^2}{\delta\langle\sigma_n\rangle\delta\langle\sigma_{n'}\rangle}$$
$$\times\left(\frac{\delta G(m,m|\omega_p)}{\delta u_m}-\langle\sigma_m\rangle G(m,m|\omega_p)\right). \quad (4.12)$$

Equation (4.12) provides a formal solution for $\phi(n,n')$ in terms of the propagator G. Substituting the CPA expressions for G, we have a result for $\phi(n,n')$ that is exact to first order in x and Z^{-1}. It remains to perform the frequency sum and integrate with respect to the multidimensional variable v_m. A simple expression is available only if just

the leading terms in δ are retained

$$\phi(n,n')=(1-\delta_{nn'})\delta^2\sum_{\omega_p}e^{\omega_p 0^+}G(n,n'|\omega_p)G(n,n'|\omega_p) \quad (4.13a)$$

$$=(1-\delta_{nn'})\delta^2\int\frac{A(n,n'|\omega_1)A(n,n'|\omega_2)}{\omega_1-\omega_2}$$
$$\times\left(\frac{1}{e^{\beta a(\omega_2-\mu_F)}+1}-\frac{1}{e^{\beta a(\omega_1-\mu_F)}+1}\right)\,d\omega_1\,d\omega_2, \quad (4.13b)$$

where $A(n,n'|\omega)$ is the usual spectral density and satisfies

$$G(n,n'|\omega_p)=\int_{-\infty}^\infty\frac{A(n,n'|\omega)}{\omega_p-\omega}\,d\omega. \quad (4.14)$$

Because typical values of kT_a are much smaller than the relevant electron energies, $A(n,n'|\omega)$ may be replaced by its zero-temperature limit. It should be noted that the appearance of the Fermi factors in (4.13) implies that the actual value of $\phi(n,n')$ depends on the (previously irrelevant) electron density. If, for example, the chemical potential μ_F lies between the host and impurity subbands, ϕ is $O(e^{-\delta/kT a})$ and is vanishingly small. This conclusion is expected to be independent of the approximations used to derive (4.13) from the exact equation (4.12). In the event that μ_F lies in a region of finite density of states the integrals in (4.13) are well behaved and the resulting expression for $\phi(n,n')$ is no greater than $O(\delta^2/Z^2)$.

Having derived an approximate expression for $\phi(n,n')$, it is now possible to include the effects of short-range order in a calculation of the electron self-energy. In particular, the off-diagonal character of $C(n_1,\ldots,n_l)$ implies that there are corrections of order x^2 to each of the diagrams in the first column of Fig. 2. Combining Eqs. (4.8) and (4.13), the higher cumulants may be approximated as

$$C(n_1,\ldots,n_l)=x^2\delta^l\delta_{nn'}\sum_{i=3}^l\prod_{j=3}^{i-1}[\delta_{n_1 n_l}+\delta_{n_i n_l}]$$
$$\times\phi(n_i,n_1)\prod_{k=i+1}^l\delta_{n_i n_k}+x^2\delta^l\phi(n_1,n_2)\prod_{k=3}^l[\delta_{n_k n_1}+\delta_{n_k n_2}]. \quad (4.15)$$

In the first term we understand that formally

$$\prod_{l=3}^2=\prod_{k=l+1}^l\equiv 1.$$

The correction of order x^2 to the lth diagram is obtained by multiplying (4.15) by $G(n_1,n_3)G(n_3,n_4),\ldots,$ $G(n_l,n_2)$ and summing on $n_3\to n_l$. After some rearrangement, this addition to the self-energy may be written as

$$\left(\frac{x^2\delta^2 G(n,n')\phi(n,n')}{(1-\delta F)^2 - \delta^2\Gamma_{nn'}}\right)(1-\delta_{nn'}) + \frac{x^2}{(1-\delta F)}\left(\sum_{m\neq n}\frac{\delta^3\phi(n,m)\Gamma_{nm}}{(1-\delta F)^2 - \delta^2\Gamma_{nm}}\right)\delta_{nn'}$$

$$= \delta^2\sum_{\omega_p}e^{\omega_p 0^+}\left(\frac{x^2 t^2 G(n,n'|\omega_p)G(n,n'|\omega_p)G(n,n')}{1-t^2\Gamma_{nn'}}(1-\delta_{nn'}) + \sum_{m\neq n}\frac{x^2 t^3 G(n,m|\omega_p)G(n,m|\omega_p)\Gamma_{nm}}{1-t^2\Gamma_{nm}}\delta_{nn'}\right).$$

$$(4.16)$$

This result is seen to be structurally similar to the naive x^2 corrections discussed at the end of Sec. III, the only difference being that two of the factors of G in the numerators of (4.16) are energy independent. To order x^2, the existence of short-range order in the alloy serves to enhance the effects of two-atom clusters. The appearance of t in Eq. (4.16) rather than Δ is an indication of the fact that our approximation (4.13) is *not* exact to any order in the parameter Z^{-1}. Any errors in the calculation of ϕ appear only in the numerator of (4.16). Zero-temperature values of G may be used in (4.16) at the expense of errors on the order of kT_a/δ.

APPENDIX A: CPA AS SOLUTION OF ORDINARY DIFFERENTIAL EQUATION

The CP equation may be rewritten as

$$V = \frac{\langle\epsilon\rangle + VF\delta}{1+VF} = \langle\epsilon\rangle + \frac{y\delta VF}{1+VF}$$

$$= \langle\epsilon\rangle + \frac{xy\delta^2 F}{(1+VF)[1-(\delta-V)F]} \quad . \quad (A1)$$

To verify that (2.32) is indeed a solution of Eqs. (2.33), we differentiate the former equation with respect to u:

$$\frac{dV}{du} = \frac{xy\delta^2}{1-(\delta-V)F} + \frac{\langle\epsilon\rangle}{[1-(\delta-V)F]^2}$$

$$\times[(\delta-V)F-1]F\frac{dV}{du}$$

$$= \frac{xy\delta^2}{1-(\delta-V)F} - VF\frac{dV}{du}$$

$$= \frac{xy\delta^2}{(1+VF)[1-(\delta-V)F]} \quad . \quad (A2)$$

The first of these equations makes use of (2.33b) as well as the fact that $d\langle\epsilon\rangle/du = c^{(2)}(x)\delta^2 = xy\delta^2$.

Comparing (A1) and (A2) we see that V satisfies

$$V = \langle\epsilon\rangle + F\frac{dV}{du}$$

in agreement with (2.33a).

APPENDIX B: EVALUATION OF $\delta V_n^{(0)}/\delta u_n$

In the lowest approximation [i.e., $V(n,n) \to V_n^{(0)}$] Eqs. (3.7) imply that $V_n^{(0)}$ satisfies the equation

$$V_n^{(0)} = \frac{\langle\epsilon\rangle[1+V_n^{(0)}G(n,n)]}{1-(\delta-\langle\epsilon_n\rangle - V_n^{(0)})G(n,n)} \quad . \quad (B1)$$

Differentiation with respect to u_n, yields

$$\frac{\delta V_n^{(0)}}{\delta u_{n'}} = \frac{\langle\epsilon_n\rangle[V_n^{(0)}\delta G(n,n)/\delta u_{n'} + G(n,n)\delta V_n^{(0)}/\delta u_{n'}]}{1-(\delta-\langle\epsilon_n\rangle - V_n^{(0)})G(n,n)}$$

$$+ \frac{\langle\epsilon\rangle[1+V_n^{(0)}G(n,n)]}{[1-(\delta-\langle\epsilon_n\rangle - V_n^{(0)})G(n,n)]^2}[(\delta-\langle\epsilon_n\rangle - V_n^{(0)})$$

$$\times \delta G(n,n)/\delta u_{n'} - (\delta V_n^{(0)}/\delta u_{n'})G(n,n)]. \quad (B2)$$

This equation expresses $\delta V_n^{(0)}/\delta u_{n'}$ in terms of $\delta G(n,n)/\delta u_{n'}$. The latter quantity serves to introduce the off-diagonal matrix elements of G. Recalling that the self-energy $V_n^{(0)}$ is site-diagonal we have

$$\delta G(n,n)/\delta u_{n'} = G(n,m)(\delta V_m^{(0)}/\delta u_{n'})G(m,n) \quad (B3)$$

$$\simeq G(n,n')(\delta V_n^{(0)}/\delta u_{n'})G(n',n)$$

$$+ G(n,n)(\delta V_n^{(0)}/\delta u_{n'})G(n,n). \quad (B4)$$

In the second line only those contributions that are of second order in the off-diagonal part of G have been retained. Substitution of (B4) into (B2) yields

$$\frac{\delta V_n^{(0)}}{\delta u_{n'}} = \frac{\langle\epsilon_n\rangle[1+V_n^{(0)}G(n,n)](\delta-V_n^{(0)})}{[1-(\delta-\langle\epsilon\rangle - V_n^{(0)})G(n,n)]^2}\Gamma_{nn'}\frac{\delta V_{n'}^{(0)}}{\delta u_{n'}}$$

$$= xy\Delta^2\Gamma_{nn'}\frac{\delta V_{n'}^{(0)}}{\delta u_{n'}} , \quad (B5)$$

where we have made use of the relation $\delta - V_n^{(0)} = y\delta[1+V_n^{(0)}G(n,n)]^{-1}$ and the definition $\Gamma_{nn'} \equiv G(n,n') \times G(n',n)$.

Equation (B5) expresses $\delta V_n^{(0)}/\delta u_{n'}$ in terms of $\Gamma_{nn'}$ and the diagonal derivative $\delta V_{n'}^{(0)}/\delta u_{n'}$. Ne-

glecting off-diagonal contributions, the latter quantity is given by

$$\delta V_n^{(0)}/\delta u_{n'} = xy\delta^2/[\,1 - (\delta - \langle \epsilon_{n'}\rangle - V_{n'}^{(0)})\,G(n',n')]$$

$$= xy\,\delta\Delta. \qquad (B6)$$

Combining (B6) and (B5), we obtain the final expression

$$\delta V_n^{(0)}/\delta u_{n'} = x^2 y^2 \Delta^3 \delta\Gamma_{nn'}$$

in agreement with (3.9) and (3.10).

[1] B. Velický, S. Kirkpartick, and H. Ehrenreich, Phys. Rev. 175, 747 (1968).
[2] P. Soven, Phys. Rev. 178, 9936 (1969).
[3] P. Soven, Phys. Rev. 156, 809 (1967).
[4] Y. Onodera and Y. Toyozawa, J. Phys. Soc. Japan 24, 341 (1968).
[5] F. Yonezawa, Progr. Theoret. Phys. (Kyoto) 40, 734 (1968).
[6] R. N. Aiyer, R. J. Elliott, J. A. Krumhansl, and P. L. Leath, Phys. Rev. 181, 1006 (1969).
[7] P. L. Leath, Phys. Rev. B 2, 3078 (1970).
[8] K. Freed, and M. H. Cohen, Phys. Rev. B 3, 3400 (1971).
[9] M. Lax, Rev. Mod. Phys. 23, 289 (1951).
[10] J. L. Beeby and S. F. Edwards, Proc. Roy. Soc. (London) A274, 395 (1962).
[11] J. L. Beeby, Phys. Rev. 13, A130 (1964).
[12] P. Soven, Phys. Rev. 151, 539 (1966).
[13] The importance of the parameter Z^{-1} was first pointed out by Professor J. Hubbard (private communication).
[14] A convenient review of functional derivative techniques may be found in L. P. Kadanoff and G. Baym, Quantum Statistical Mechanics (Benjamin, New York, 1962).
[15] P. L. Leath, Phys. Rev. 171, 725 (1968).
[16] R. Kubo, J. Phys. Soc. Japan 17, 1100 (1962).
[17] L. Schwartz, F. Brouers, A. V. Vedyayev, and H. Ehrenreich, Phys. Rev. B 4, 3383 (1971).
[18] D. W. Taylor, Phys. Rev. 156, 1017 (1967).
[19] P. L. Leath, Phys. Rev. B 2, 3078 (1970).
[20] F. Yonezawa and T. Matsubara, Progr. Theoret. Phys. (Kyoto) 35, 759 (1966).
[21] V. Čápek, Phys. Status Solidi 43, 61 (1971).
[22] F. Cyrot Lackmann and F. Ducastelle, Phys. Rev. Letters 27, 429 (1971).
[23] T. Wolfram and J. Callaway, Phys. Rev. 130, 2207 (1963).
[24] Equation (3.17) is closely related to the pair equations of Freed and Cohen (Ref. 8) and Cyrot Lackmann and Ducastelle (Ref. 22). Equivalent results were previously discussed by L. Schwartz, Ph.D. thesis (Harvard University, 1970) (unpublished).